Stochastic Ground Motion Simulations for Assessment of Regional Losses from Induced Earthquakes

Taojun Liu[a], Nicolas Luco[b], Abbie B. Liel[c] and Sanaz Rezaeian[d]

[a]Research Associate, University of Colorado Boulder; Visiting Scholar, United States (U.S.) Geological Survey
[b]Research Structural Engineer, United States (U.S.) Geological Survey
[c]Associate Professor, University of Colorado Boulder
[d]Research Structural Engineer, United States (U.S.) Geological Survey

Abstract: In this study, we propose a stochastic ground motion simulation framework that explicitly considers the spatial correlation of ground motions and thereby is suitable for regional seismic risk assessment. We first investigate the spatial correlation characteristics of the simulation parameters; based on estimated simulation parameters and their spatial correlations using ground motion records from Chi-Chi earthquake, we then present a simulation example to illustrate the importance of incorporating the spatial correlation of the simulation parameters. Future work will apply the framework in risk assessment from induced earthquakes.

1 Introduction

Earthquake rates for portions of the Central and Eastern United States (CEUS) have increased dramatically since about 2009. The majority of these earthquakes are classified as induced because they are considered to be related to wastewater injection during oil and gas production, rather than tectonic activities [12]. Quantitative seismic loss assessment is needed to address the risks posed by these frequent, potentially damaging earthquakes. Since historical ground motion records that match the possible future earthquake scenarios in this region are not available, simulated records can be adopted to evaluate the seismic loss potential. For ground motion simulation, we adopt a stochastic approach, recognizing the lack of detailed geophysical information for the CEUS [13]. The simulated ground motion records capture the intensity, duration, spectral content and peak values of actual ground motions, through use of parameters that characterize the evolving intensity, predominant frequency and bandwidth of the ground motion records. In addition to losses to individual buildings and infrastructure, stakeholders are interested in understanding the seismic loss for the types of events that have and could occur over the region. A number of studies [1, 2, 5, 9, 11] have demonstrated that the spatial correlation in ground motions can significantly affect the outcome of seismic loss estimates for spatially distributed structures/infrastructure. This finding emphasizes the importance of incorporating the spatial correlation characteristics of ground motions in the simulation approach.

In this paper, we work towards a regional seismic loss assessment for a portfolio of buildings located in a CEUS city subjected to several induced earthquakes. As the first step towards this goal, in this study we develop a stochastic ground motion simulation framework that specifically considers spatial correlations between simulation parameters that is suitable for regional seismic risk assessment in this region. Specifically, we first estimate spatial correlation characteristics between the simulation parameters using ground motion records from the 1999 Chi-Chi earthquake. This event is very well recorded, with about 400 records available in the

PEER NGA database. In addition, a number of researchers [3, 4, 6, 8] have studied the spatial correlation characteristics of ground motion parameters (e.g., peak ground acceleration, PGA; spectral acceleration, SA; and Arias intensity, I_A) based on these records; here, we extend these studies to the other ground motion parameters needed for the stochastic simulation. As an illustration, we then present an example with simulated ground motion records for 5 sites based on the estimated simulation parameters and their spatial correlation characteristics. Finally, we also explore the use of stochastic simulation parameters to characterize the recorded ground motions from an induced earthquake ground motion database. These efforts lay the groundwork for a more extensive and systematic study of the simulation parameters and spatial correlation characteristics that will make possible simulation of more realistic ground motions, and consequently improve the accuracy of regional loss estimation.

2 Stochastic Ground Motion Simulation Framework for Regional Seismic Risk Assessment

2.1 Stochastic Ground Motion Simulation Approach and its Parameters

The stochastic ground motion simulation approach developed by Rezaeian and Der Kiureghian [13] is employed here. This nonstationary stochastic approach provides a convenient method of generating synthetic ground motions that have characteristics similar to those of real earthquake ground motions. The simulated ground motion can be thought of as white noise excitation filtered through a linear single-degree-of-freedom oscillator with evolving vibration frequency and a time modulation function to achieve spectral and temporal nonstationarity.

In this approach, ground motions are characterized by 6 model parameters that have physical interpretations: 3 parameters define the time modulation function and 3 parameters control the evolving predominant frequency and bandwidth of the ground motion. The time modulation function $q^2(t, \boldsymbol{\alpha})$ can be written as proportional to a gamma probability density function:

$$q^2(t, \boldsymbol{\alpha}) = \alpha_1^2 t^{(2\alpha_2 - 1) - 1} exp(-2\alpha_3 t) \tag{1}$$

where α_1, α_2 and α_3 are model parameters that are related to the Arias intensity, I_A; the significant duration, $D_{5\text{-}95}$, defined as the time between 5% to 95% of I_A; and the time to the middle of the strong ground motion phase, t_{mid}, defined as the time to reach 45% of I_A. The spectral nonstationarity is controlled by ω_{mid}, the filter frequency at t_{mid}, and ω', the rate of change of the filter frequency with time; the bandwidth (of the ground motion) is defined by the damping ratio of the filter, ζ_f.

The stochastic simulation approach starts with a set of seed motions representative of the seismic environment of interest. Once the 6 model parameters are identified for each seed record, marginal probability distributions are assigned to each parameter based on the observations in the seed record set. To relate the model parameters to an earthquake scenario, an empirical regression that is analogous to a ground motion prediction equation can be developed for each model parameter. To facilitate the development of these regressions, the stochastic model parameters are transformed to standard normal space, based on the empirical marginal cumulative distribution for each, and denoted as v_i (i = 1, 2, … 6). The standard deviation associated with each regression represents the uncertainty in the model parameter that captures its variability across the simulated ground motions.

To simulate ground motion records for an earthquake scenario, one can randomly sample the transformed model parameters v_i (i = 1, 2, … 6) based on the prediction equations. Then, v_i are transformed back to the original model parameter space (I_A, $D_{5\text{-}95}$, t_{mid}, ω_{mid}, ω', ζ_f) according to their fitted marginal probability distributions. The time modulation functions and the white noise filter can then be determined and, hence, the ground motions can be generated. This procedure is repeated multiple times to obtain a suite of simulated ground motions.

2.2 Spatial Correlation Characteristics of Simulation Parameters

The simulation procedure in the previous section is generally oriented toward ground motion simulation at a single site, where the potential correlations between model parameters for spatially distributed sites can be ignored. As a result, we expect the simulated ground motion may not be consistent with observed spatial correlation characteristics. If such simulations are adopted in seismic risk assessment of spatially distributed assets, as shown by previous studies [5, 9, 11], the aggregate loss estimate will be biased. In the following, we develop spatial correlation models for each simulation parameter based on historical ground motion records from the 1999 Chi-Chi earthquake. These can be integrated into the simulation procedure by developing spatial correlation models that can be used when randomly sampling the model parameters for the simulation at each site. Spatial correlations among each model parameter for different ground motions are calculated based on the regression residuals.

2.2.1 Ground Motion Records

The ground motion records from the 1999 Chi-Chi earthquake obtained from the PEER NGA West database [10] are adopted in this study. After discarding poor-quality data recorded with older-type instruments, we selected a total of 389 ground motion records. This is the same dataset used in a previous study focused on spatial correlation of PGA and SAs [7]. The surface projection of the finite fault and the spatial distribution of the selected records shown in Figure 1(a) indicates very good coverage over the island of Taiwan and varying source-to-site distances.

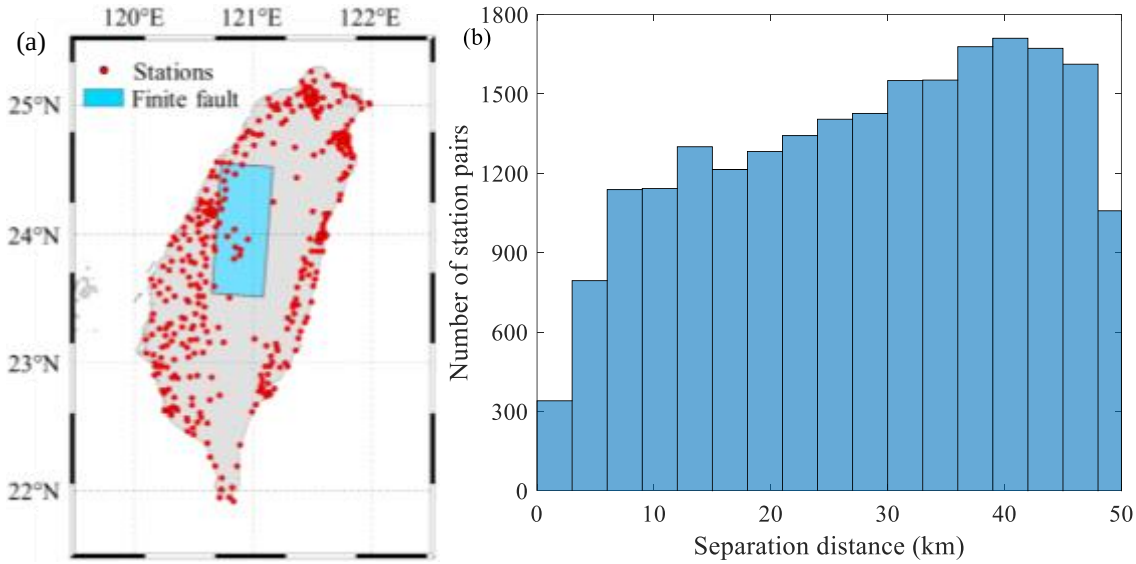

Figure 1: Selected ground motion records from the 1999 Chi-Chi earthquake: (a) locations of recording stations and surface projection of the finite fault model; (b) histogram of separation distance within 50 km.

For the analysis that follows, we consider each horizontal component as a randomly-oriented record to increase the number of samples. Based on this consideration, we show in Figure 1(b) a histogram for the separation distances between station pairs that are less than or equal to 50 km. A maximum of 50 km is considered in previous studies [4, 7, 8] as the cut-off distance because the spatial correlations for ground motion parameters (PGA, SA and I_A) beyond this value is negligible. Generally, there are more than 1000 pairs of stations within a 3 km bin for separation distances greater than about 5 km. Even at very close distances (less than about 5 km), each bin contains more than 300 data pairs.

2.2.2 Prediction Models for Simulation Parameters

In Table 1, we assign probabilistic distributions for each of the six simulation-model parameters based on parameter values from the ground motion records from the 1999 Chi-Chi earthquake. The parameters are estimated using the method of maximum likelihood. In general, the parameters values are in similar ranges to those reported in [13] that are based on 206 horizontal ground motion components recorded in 19 earthquakes from the NGA database. Since we are working with a large number of ground motion records from a single event, the uncertainties associated with the parameters reported in Table 1 are smaller for I_A, ω_{mid}, ω' and ζ_f compared to [13]. However, the standard deviations for duration parameters are larger, which is because the largest source-to-site distance is about 200 km, while Rezaeian and Der Kiureghian [13] used 100 km. Given this choice, the larger variability observed for the duration parameters is expected.

Table 1: Probabilistic distributions and bounds for model parameters.

Parameter	Mean	Standard Deviation	Fitted Distribution	Bounds
I_A (s.g)	0.058	0.136	Lognormal	(0, ∞)
$D_{5\text{-}95}$ (s)	33.5	13.62	Beta	[5, 140]
t_{mid} (s)	25.7	8.29	Beta	[8, 54]
$\omega_{\text{mid}}/2\pi$ (Hz)	2.58	1.227	Gamma	(0, ∞)
$\omega'/2\pi$ (Hz)	-0.046	0.0375	Two-sided Generalized Extreme Value	[-0.3, 0.2]
ζ_f	0.13	0.118	Beta	[0.01, 1]

We then develop empirical prediction equations for the model parameters v_i (i = 1, 2, … 6) in standard normal space using the functional form below:

$$v_i = c_0 + c_1 lnR + c_2 R + c_3 ln\left(\frac{V_{s30}}{V_{ref}}\right) + \varepsilon \quad i = 1,2,\dots 6 \tag{2}$$

where c_0, c_2, c_2 and c_3 are regression coefficients; V_{s30} is the average shear wave velocity of the top 30 m of soil at the recording site; $R = \sqrt{R_{rup}^2 + h^2}$, in which R_{rup} is the closest distance from the recording site to the fault rupture plane, h is a depth term that builds in near-source saturations due to finite-fault effects, and ε is the residual. The value of h is determined by searching within the range from 1 to 10 km to find the value that minimizes the standard deviation of the residuals. We set V_{ref} = 760 m/s. The regression coefficients and the standard deviation of the residuals are listed in Table 2 for the transformed model parameters. Plots of residuals, which are excluded from this paper to save space, do not show any apparent trend with respect to source-to-site distance or site condition.

The regression analysis reveals some insights into the model parameters. For example, Arias intensity decreases with distance and site stiffness (V_{s30}); the duration parameters ($D_{5\text{-}95}$ and t_{mid}) tend to increase with distance, but decrease with site stiffness; the filter damping ratio, ζ_f, decreases with source-to-site distance. These trends are consistent with those reported in [13]. We adopted two distance terms (c_1 and c_2) in the functional form (Eq. 2). However, the second term (coefficient c_2) is not significant except for ω_{mid} and ω'. The use of two distance terms is advantageous for these two parameters because we are able to model the change of attenuation patterns with distance for ω_{mid} and ω'. The values of ω_{mid} increase with distance up to about 40 km, then decrease; while ω' is the opposite, decreasing with distance up to about 40 km then increase. In general, the standard deviations are similar to those in [13] except for duration parameters, which is because the use of larger source-to-site distance, as mentioned above.

Table 2: Regression coefficients for the prediction models for transformed model parameters

Parameter	h (km)	c_0	c_1	c_2	c_3	σ_ε
v_1 (I_A)	5.9	3.09	-0.837	-0.00439	-0.622	0.580
v_2 ($D_{5\text{-}95}$)	1	-1.54	0.169	0.000383	-1.11	0.846
v_3 (t_{mid})	1	-2.27	0.359	0.00644	-0.605	0.746
v_4 ($\omega_{\text{mid}}/2\pi$)	10	-1.12	0.947	-0.0302	0.865	0.767
v_5 ($\omega'/2\pi$)	1	1.12	-0.643	0.0138	-0.619	0.928
v_6 (ζ_f)	10	2.37	-0.505	-0.00703	-0.121	0.795

2.2.3 Spatial Correlation Characteristics of Model Parameters

Based on the developed prediction equations and the associated residuals, we investigate the spatial correlation characteristics of model parameters. From a recorded earthquake (Chi-Chi in this study), the spatial correlation coefficient for each model parameter can be computed analogously with that for other ground motion intensities (e.g., SA), as

$$\rho_\epsilon(\Delta) = 1 - \frac{[\sigma_d(\Delta)]^2}{2(\sigma_\epsilon)^2}, \tag{3}$$

where Δ is the separation distance between the j-th and k-th recording stations, $[\sigma_d(\Delta)]^2$ is the variance of $\epsilon_j - \epsilon_k$, where ϵ_j is the residual with respect to a ground motion prediction equation for the model parameter that is developed previously, and σ_ϵ is the standard deviation of ϵ_j. This calculation is carried out within each 3 km bin (Figure 1b).

Figure 3 shows the calculated spatial correlation coefficients and the fitted exponential model $\rho_\epsilon(\Delta) = \exp(-\alpha\Delta^\beta)$ for the transformed model parameters. The correlation coefficient for Arias intensity shown in Figure 3a is very similar to that of SA at 1.0 s [7]. Although different subset of ground motions from the Chi-Chi earthquake and different prediction equations are used, this correlation closely matches the result of [3] for separation distance less than 50 km by converting their semivariogram to correlation coefficients.

The spatial correlations of duration parameters v_2 ($D_{5\text{-}95}$) and v_3 (t_{mid}) are generally higher in comparison with Arias intensity and other ground motion parameters. However, they show different characteristics. For v_2 ($D_{5\text{-}95}$), the spatial correlation is relatively low, even for closely spaced sites (about 0.6 for separation distance less than 5 km); yet, the spatial correlation decreases slowly with separation distance with value of 0.4 at 50 km for the fitted model. Nevertheless, since the correlation coefficient equals unity at zero separation by definition, the same exponential functional form is used to fit the spatial correlations of v_2. On the other hand,

the spatial correlations for $v_3(t_{\mathrm{mid}})$ is very high (> 0.8) at short separation distance and decays faster to about 0.3 at 50 km.

The spatial correlations for v_4 (ω_{mid}), v_5 (ω') and v_6 (ζ_f) are rather low, especially for v_4 and v_6. In general, the correlation coefficient is less than 0.2 for separation distance larger than 10 km. For v_5, the correlation coefficient is less than 0.2 for separation distance larger than about 20 km. Although one may ignore correlations below 0.2 in practical applications, we apply spatial correlations for the full range of separation distance until later analysis supports further simplification.

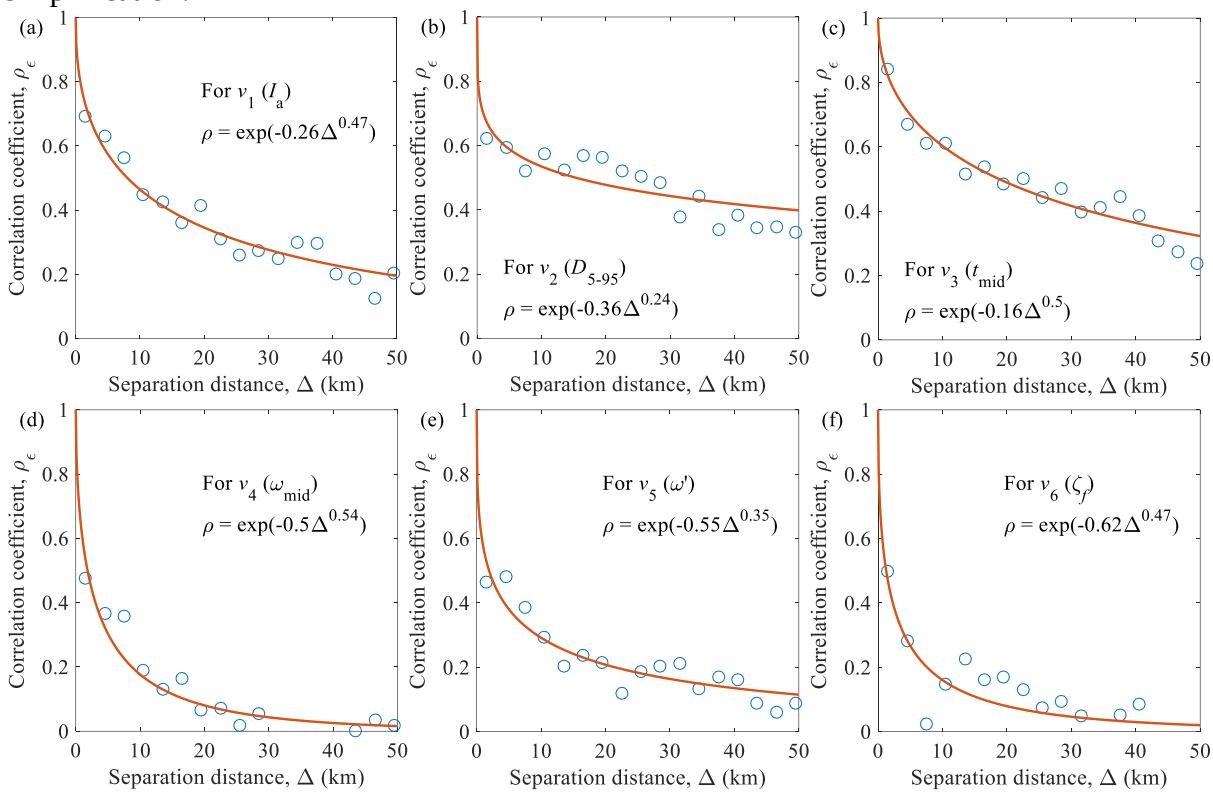

Figure 3: Empirical spatial correlations and the fitted model for the transformed model parameters.

2.2.4 Correlation Coefficients between Model Parameters

As investigated by Rezaeian and Der Kiureghian [13], the transformed model parameters are not independent. We calculate the correlation coefficients between the transformed model parameters and list them in Table 3. These correlation coefficients are generally similar to those reported in [13], which are based on ground motions from multiple events. For example, v_1 (I_A) is negatively correlated with duration parameters v_2 ($D_{5\text{-}95}$) and v_3 (t_{mid}), indicating the motions with high amplitude tend to have shorter durations, because Arias intensity is more strongly related to the amplitude of the motion than to the duration. As expected, v_2 ($D_{5\text{-}95}$) and $v_3(t_{\mathrm{mid}})$ are highly correlated. The negative correlation between v_4 (ω_{mid}) and v_5 (ω') indicates that motions with higher predominant frequency tend to have a faster decay of the frequency with time. The correlation between v_5 (ω') and v_6 (ζ_f) is negative and relatively significant, suggesting a faster decay of the frequency with time tends to imply a broader bandwidth. The correlations between some model parameters are very low and can be ignored for practical applications. However, the cut off value for the correlation cannot be arbitrarily determined without justification, and we use the full correlation matrix in the section to follow.

Table 3: Sample correlation coefficients between transformed model parameters.

	v_1	v_2	v_3	v_4	v_5	v_6
v_1	1	-0.31	-0.38	-0.11	0.05	-0.02
v_2		1	0.68	-0.21	0.20	-0.04
v_3			1	-0.20	0.05	-0.09
v_4				1	-0.46	0.10
v_5		*Symmetric*			1	-0.29
v_6						1

3 Simulation Example

Based on the empirical prediction equations for the simulation parameters and their spatial correlation characteristics, we simulate ground motions at 5 hypothetical sites for Chi-Chi earthquake. These sites are assumed to be located at uniform site condition with V_{s30} = 760 m/s and rupture distances of 50 km, 52 km, 60 km, 65 km and 70 km. The schematic layout of the sites is shown in Figure 4a. For simplicity, the separation distance between a pair of sites is assumed to be the difference between their rupture distances. This is true if the closest point on the fault to the stations is on the west fault edge with zero depth. The simulations with and without spatial correlations of the model parameters are repeated for 100 times each case. Figure 4(b) plots the simulated ground motions examples, showing that the simulated ground motions are similar to each other if the spatial correlations between model parameters are considered (left column). On the other hand, visual inspection of the accelerograms in the right column of Figure 4(b) shows that the characteristics of the simulated ground motions can be very different from site to site.

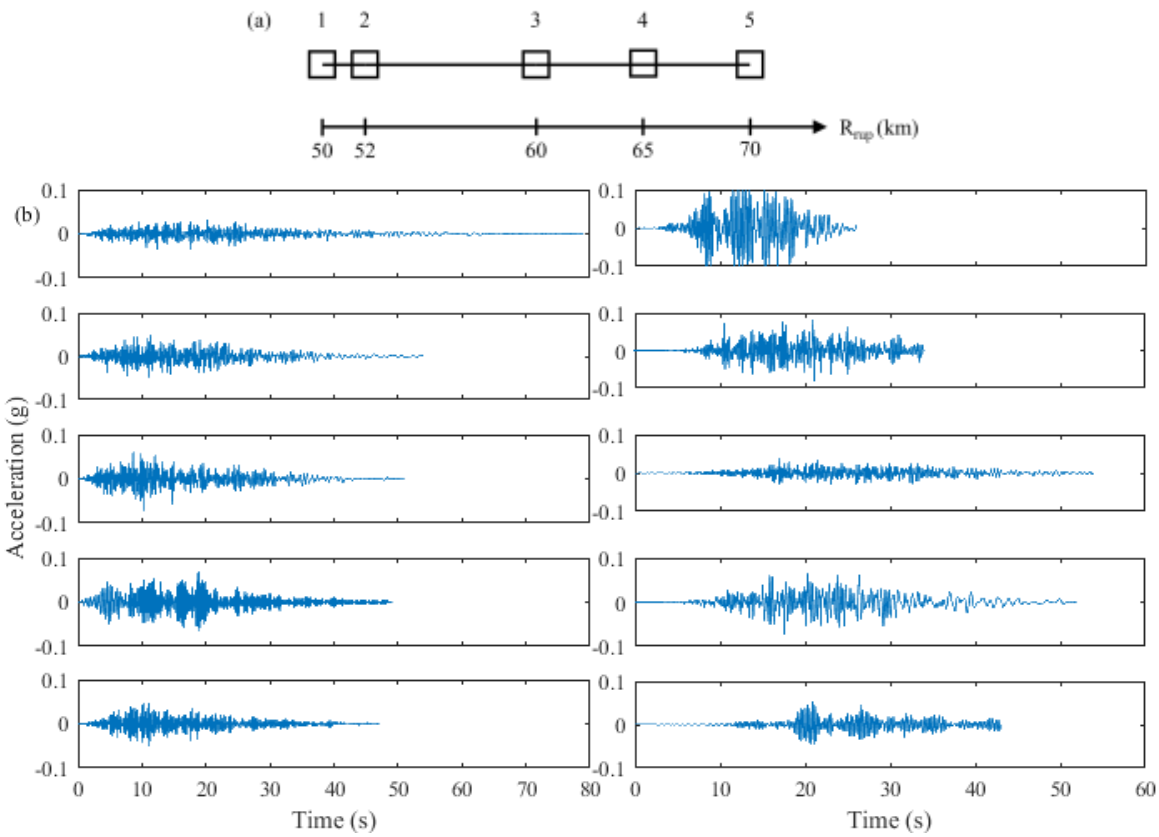

Figure 4: (a) Schematic layout of 5 hypothetical sites; and (b) sample simulations: left column results from spatially correlated model parameters, right column simulations ignore spatial correlation of the parameters.

Now we examine if including the spatial correlations between model parameters will produce spatially correlated spectral acceleration (SA) consistent with observations from actual recorded ground motions. In Figure 5 we show the calculated spatial correlation coefficients from the simulated ground motions with or without considering the spatial correlations between model parameters, and compare these with the observed spatial correlations of SAs at 0.3 s and 3.0 s. The observations are based on the fitted exponential spatial correlation models are developed previously using the Chi-Chi ground motions [7]. First, the spatial correlation coefficients for SA without considering spatial correlations of model parameters are essentially zero, which is expected since only the correlations between the parameters at the same site (Table 3) are considered. Second, by using spatially correlated model parameters, the spatial correlations of SAs increases. The increased correlations generally decrease with increasing separation distance. However, the SAs from these simulations are not as highly correlated as that observed in the Chi-Chi earthquake, indicating that ignoring the cross correlation between different parameters at different sites (e.g., between I_A and $D_{5\text{-}95}$ at different locations) leads to insufficient correlations in the simulated ground motions. We will investigate the spatial cross correlations of simulation model parameters in the near future.

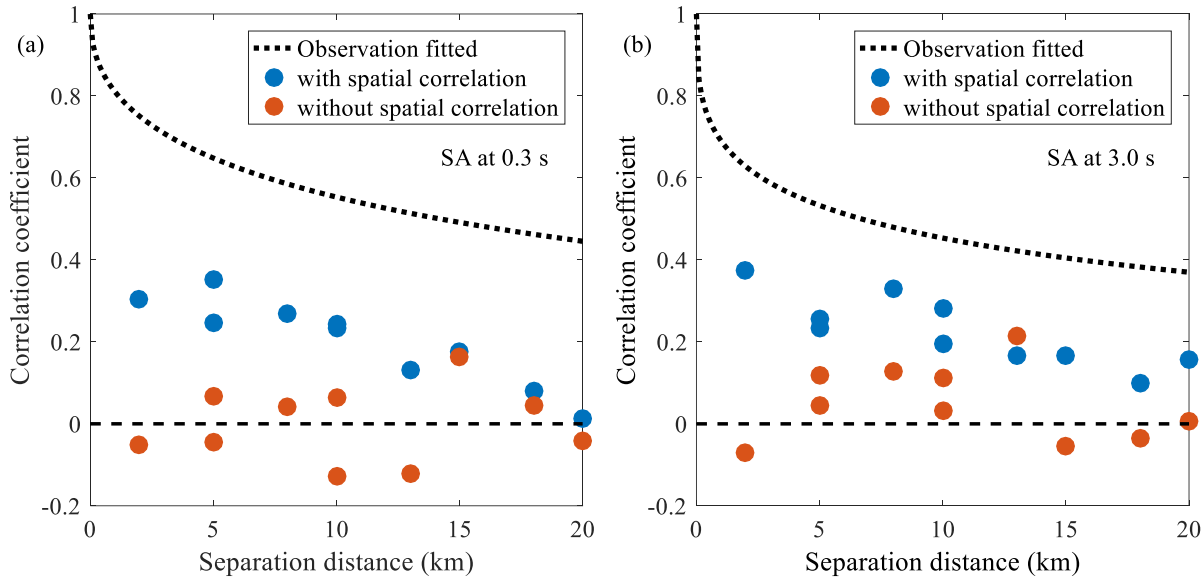

Figure 5: Comparison of spatial correlation coefficent for the simulated ground motions with or without considering spatial correlation between model parameters: (a) for SA at 0.3 s; (b) for SA at 3.0 s.

4 Exploration of Induced Ground Motions Characteristics

In this section, we explore the characteristics of ground motions from induced earthquakes. We select 50 ground motion records with the largest PGA values from a database of ground motions from induced earthquakes compiled by Rennolet et al. [12]. These records are from 33 earthquakes with magnitude ranges from 3.0 to 4.8. This database contains more than 100,000 ground motions from Oklahoma and Southern Kansas recorded between November, 2011 and March, 2016. The records are processed following the procedures described for the NGA-West2 ground motion database, along with additional steps to check for record clipping and modifications to the signal window to account for high seismicity rates in the region. Using the selected records from induced earthquakes, we summarize the probabilistic distributions of the simulation model parameters in Table 4.

Comparison of the results reported in Table 4 with those in Table 1 and [13] reveals some characteristics of induced ground motions that are fairly different from tectonic ground motions. Specifically, the energy (I_A) contained by these motions is small; durations ($D_{5\text{-}95}$ and t_{mid}) are shorter; predominate frequency (ω_{mid}) is higher; change of frequency with respect to time (ω') is faster. However, the bandwidth (ζ_f) is similar. These differences may be dependent on the earthquake magnitude since ground motions from large earthquake tends to be stronger and have longer duration and richer low frequency content. Moreover, the relative uncertainties of the model parameters are generally larger because the results for induced motions are derived based on 100 ground motion components. Future studies are deserved to examine the unique features from induced ground motions.

Due to the limited spatial coverage of recording stations from induced earthquakes, the attempt to investigate the spatial correlation characteristics of induced ground motions lead to unstable results. This lack of records is also true for tectonic earthquakes in the Central and Eastern U.S. Given this situation, the empirical spatial correlation models for the stochastic simulation model parameters developed in this study may be used.

Table 4: Probabilistic distributions and bonds for model parameters for ground motions from induced events.

Parameter	Mean	Standard Deviation	Fitted Distribution	Bounds
I_A (s.g)	0.0083	0.013	Lognormal	(0, ∞)
$D_{5\text{-}95}$ (s)	2.74	3.20	Beta	[0.19, 21]
t_{mid} (s)	1.40	0.90	Beta	[0.45, 6.5]
$\omega_{\text{mid}}/2\pi$ (Hz)	14.56	4.28	Gamma	(0, ∞)
$\omega'/2\pi$ (Hz)	-1.78	2.82	Two-sided Generalized Extreme Value	[-13, 3]
ζ_f	0.17	0.18	Beta	[0, 0.9]

5 Conclusions

We present a stochastic ground motion simulation framework that is capable of simulating ground motions with realistic spatial correlation characteristics. The simulated ground motion records are developed for use as ground motion excitations in regional seismic loss assessment. Spatial correlation characteristics of the simulation parameters are computed based on records from the well-recorded 1999 Chi-Chi earthquake. The results suggest that the spatial correlation of Arias intensity (I_A), significant duration ($D_{5\text{-}95}$), time to the middle of the strong ground motion phase (t_{mid}) and the rate of change of the filter frequency with time (ω'), should be considered in the simulation. On the other hand, filter frequency at t_{mid} (ω_{mid}) and the damping ratio of the filter (ζ_f) for spatially distributed locations with separation distance larger than 10 km may be considered independent for practical applications. Example simulations illustrate the importance of including such correlations. However, ignoring the spatial cross correlations of simulation model parameters leads to unsatisfactory spatial correlations between spectral accelerations, which is an issue for future investigation. We also examine a limited number of ground motions from induced earthquakes whose characteristics differ from that of strong tectonic ground motions, as quantified by the parameters in the simulation approach. Future work is needed to systematically study induced ground motions and develop empirical models that can be incorporated in the proposed framework in order to conduct regional seismic loss estimation under induced earthquakes.

Acknowledgement

This material is based upon work supported by the National Science Foundation under Grant No. 1520846. Any opinion, findings, and conclusions or recommendations expressed in this material are those of the author(s) and do not necessarily reflect the views of the National Science Foundation. In addition, Taojun Liu would like to acknowledge the postdoctoral fellowship awarded by the Natural Sciences and Engineering Research Council of Canada.

References

[1] Crowley, H., & Bommer, J. J. (2006). Modelling seismic hazard in earthquake loss models with spatially distributed exposure. *Bulletin of Earthquake Engineering*, *4*(3), 249-273.

[2] DeBock, D. J., & Liel, A. B. (2015). A comparative evaluation of probabilistic regional seismic loss assessment methods using scenario case studies. *Journal of Earthquake Engineering*, *19*(6), 905-937.

[3] Foulser-Piggott, R., & Stafford, P. J. (2012). A predictive model for Arias intensity at multiple sites and consideration of spatial correlations. *Earthquake Engineering & Structural Dynamics*, *41*(3), 431-451.

[4] Goda, K., & Hong, H. P. (2008a). Spatial correlation of peak ground motions and response spectra. *Bulletin of the Seismological Society of America*, 98(1), 354-365.

[5] Goda, K., & Hong, H. P. (2008b). Estimation of seismic loss for spatially distributed buildings. *Earthquake Spectra*, 24(4), 889-910.

[6] Jayaram, N., & Baker, J. W. (2009). Correlation model for spatially distributed ground-motion intensities. *Earthquake Engineering & Structural Dynamics*, 38(15), 1687-1708.

[7] Liu, T. J., Atkinson, G. M., Hong, H. P., & Assatourians, K. (2012). Intraevent spatial correlation characteristics of stochastic finite-fault simulations. *Bulletin of the Seismological Society of America*, 102, 1740-1747.

[8] Liu, T. J., & Hong, H. P. (2015). Application of spatially correlated and coherent records of scenario event to estimate seismic loss of a portfolio of buildings. *Earthquake Spectra*, 31(4), 2047-2068.

[9] Pacific Earthquake Engineering Research Center (PEER) (2010). Next generation attenuation (NGA) database, http://peer.berkeley.edu/nga/ (last accessed August 2010).

[10] Park, J., Bazzurro, P., & Baker, J. W. (2007). Modeling spatial correlation of ground motion intensity measures for regional seismic hazard and portfolio loss estimation. *Applications of statistics and probability in civil engineering. Taylor & Francis Group, London*, 1-8.

[11] Petersen, M. D., Mueller, C. S., Moschetti, M. P., Hoover, S. M., Llenos, A. L., Ellsworth, W. L., Michael, A. J., Rubinstein, J. L., McGarr A. F., & Rukstales, K. S. (2016). *2016 One-Year Seismic Hazard Forecast for the Central and Eastern United States from Induced and Natural Earthquakes* (No. 2016-1035). US Geological Survey.

[12] Rennolet, S., Moschetti, M. P., Thompson, E. M. and Yeck, W. (2016). A flatfile of ground motion measurements from induced earthquakes in Oklahoma and Kansas. Submitted to *Earthquake Spectra*.

[13] Rezaeian, S., & Der Kiureghian, A. (2010). *Stochastic modeling and simulation of ground motions for performance-based earthquake engineering*. Pacific Earthquake Engineering Research Center.